Remote electrochemical modulation of pK_a in a rotaxane by co-conformational allostery

Giulio Ragazzon[a], Christian Schäfer[a], Paola Franchi[a], Serena Silvi[a], Benoit Colasson[a,b], Marco Lucarini[a,1], and Alberto Credi[c,d,e,1]

[a]Dipartimento di Chimica "G. Ciamician," Università di Bologna, 40126 Bologna, Italy; [b]Laboratoire de Chimie et de Biochimie Pharmacologiques et Toxicologiques, CNRS UMR 8601, Université Paris Descartes Sorbonne Paris Cité, 75006 Paris, France; [c]Dipartimento di Scienze e Tecnologie Agro-alimentari, Università di Bologna, 40127 Bologna, Italy; [d]CLAN – Center for Light Activated Nanostructures, Università di Bologna and Consiglio Nazionale delle Ricerche, 40129 Bologna, Italy; and [e]Istituto per la Sintesi Organica e la Fotoreattività, Consiglio Nazionale delle Ricerche, 40129 Bologna, Italy

Edited by J. Fraser Stoddart, Northwestern University, Evanston, IL, and approved November 27, 2017 (received for review September 29, 2017)

Allosteric control, one of Nature's most effective ways to regulate functions in biomolecular machinery, involves the transfer of information between distant sites. The mechanistic details of such a transfer are still an object of intensive investigation and debate, and the idea that intramolecular communication could be enabled by dynamic processes is gaining attention as a complement to traditional explanations. Mechanically interlocked molecules, owing to the particular kind of connection between their components and the resulting dynamic behavior, are attractive systems to investigate allosteric mechanisms and exploit them to develop functionalities with artificial species. We show that the pK_a of an ammonium site located on the axle component of a [2]rotaxane can be reversibly modulated by changing the affinity of a remote recognition site for the interlocked crown ether ring through electrochemical stimulation. The use of a reversible ternary redox switch enables us to set the pK_a to three different values, encompassing more than seven units. Our results demonstrate that in the axle the two sites do not communicate, and that in the rotaxane the transfer of information between them is made possible by the shuttling of the ring, that is, by a dynamic intramolecular process. The investigated coupling of electron- and proton-transfer reactions is reminiscent of the operation of the protein complex I of the respiratory chain.

acid–base processes | electrochemistry | free energy change | molecular machine | molecular switch

Allostery—the process by which a chemical transformation at one site causes a change at a distant site within the same molecule or molecular assembly—is a key phenomenon for the regulation of biological activity (1, 2). A most important example is the long-range coupling of redox-active and acid–base-sensitive sites, a crucial element of electron transport chains, as exemplified by the respiratory complex I (3). Although allosteric effects are usually described in terms of conformational changes induced by binding at one site directly affecting the affinity of the other site (4), the idea that the transmission of information at the basis of allostery could take place through dynamic mechanisms is receiving increasing attention (5–7). Indeed, despite its importance for life, allosteric regulation remains an elusive biochemical phenomenon.

Mechanically interlocked molecules (MIMs) (8) such as rotaxanes and catenanes, because of the lack of strong chemical bonds between their molecular parts, are characterized by a rich dynamic behavior that involves changes of the relative position of the components (co-conformation). Indeed, in appropriately designed MIMs co-conformational rearrangements can be precisely controlled by modulating the noncovalent intercomponent interactions through external stimulation (9, 10). For these reasons, MIMs can be regarded as appealing systems for investigating allosteric communication mechanisms and implementing them within synthetic species to achieve functions (11). Nevertheless, studies of allosteric effects in rotaxanes and catenanes are rare (12) and have been limited so far to a pioneering work by Sauvage and coworkers (13) and, more recently, to the realization of stimuli-responsive switches (14, 15) for controlling catalytic functions (16–20).

In a recent investigation of a family of [2]rotaxanes (21) we showed quantitatively that the acidity of an ammonium ion on the axle is strongly depressed when it is surrounded by a crown ether ring, for which it is an efficient recognition motif (8). Such a phenomenon, that can be rationalized with both thermodynamic and kinetic arguments, is in line with earlier observations (22–26) that deprotonation of ammonium axles in crown ether-based rotaxanes is extremely difficult to achieve. We also found that the decrease of acid strength is mitigated in the presence of an alternative recognition site for the ring.

Building on these observations, here we investigate the possibility of manipulating the pK_a of an ammonium site located on the axle component of a [2]rotaxane by changing the affinity of a remote recognition site for the interlocked crown ether ring. The latter site is redox-active and therefore an electrochemical approach is employed. As the acid–base- and redox-active units are completely insulated from one another in the axle molecule, we aim at understanding if and how the shuttling of the ring in the rotaxane can result in the transfer of information between the distal sites. Besides the potential practical utility of electrochemical switching of acid–base properties with an unsophisticated synthetic compound, this study can shine light on allosteric effects brought about by co-conformational changes in MIMs.

Significance

Rotaxanes are species in which a macrocyclic molecule—the ring—is interlocked with a dumbbell-shaped component—the axle. The translational motion of the ring along the axle provides the basis for constructing molecular machinery. In this paper we show that such a dynamic process enables the transfer of chemical information between two distant sites; as a result, the acidity of one site can be reversibly modulated by redox switching at the other site. Possibilities emerge not only for the rational design of species with tailor-made acid–base properties but also for the development of model systems to understand some of Nature's most effective regulatory mechanisms—namely, allostery and proton-coupled electron transfer.

Author contributions: G.R. and A.C. designed research; G.R., C.S., P.F., S.S., B.C., and M.L. performed research; G.R., C.S., P.F., S.S., B.C., M.L., and A.C. analyzed data; and A.C. wrote the paper.

The authors declare no conflict of interest.

This article is a PNAS Direct Submission.

[1]To whom correspondence may be addressed. Email: marco.lucarini@unibo.it or alberto.credi@unibo.it.

This article contains supporting information online at www.pnas.org/lookup/suppl/doi:10.1073/pnas.1712783115/-/DCSupplemental.

Published online December 18, 2017.

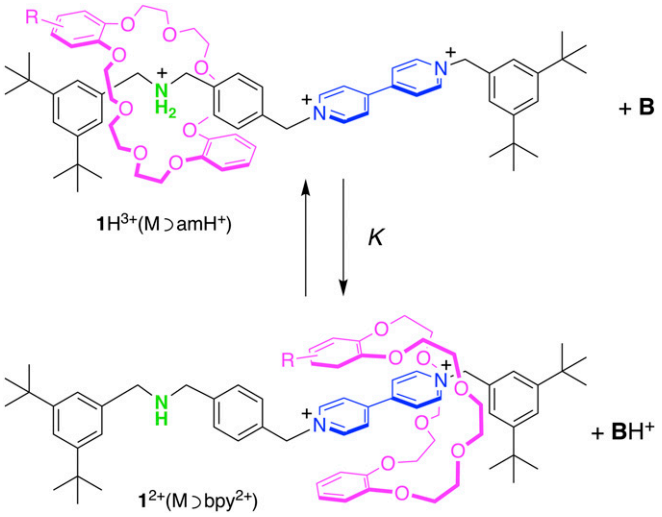

Fig. 1. Structural formula of rotaxane $\mathbf{1}H^{3+}$ in its stable (M⊃amH$^+$) co-conformation, and representation of the base (B)-induced transformation into $\mathbf{1}^{2+}$, whose stable co-conformation is (M⊃bpy^{2+}). R = $CH_2O(CH_2)_3CN$; positive charges are balanced by PF_6^- anions.

Results and Discussion

Design. The investigated rotaxane $\mathbf{1}H^{3+}$ (Fig. 1) is based on a well-known architecture (27) and was recently used to develop a molecular transporter (28). The axle component contains a dibenzylammonium (amH$^+$) and a 4,4′-bipyridinium (bpy^{2+}) unit that serve as recognition sites for a dibenzo[24]crown-8 macrocycle (M). In $\mathbf{1}H^{3+}$ the molecular ring encircles almost exclusively the amH$^+$ site; in the presence of a suitable base the rotaxane is deprotonated and M translates over the bpy^{2+} unit, where it is engaged in charge-transfer interactions (27, 29). The acid–base-controlled shuttling reaction is schematized in Fig. 1. The presence of a nitrile-terminated tether on the ring is irrelevant for the properties discussed here. Rotaxanes related to $1H^{3+}$ with different or no substituent on the crown ether ring exhibited the same switching properties (27, 28, 30). Moreover, we showed recently that the displacement of the ring along the axle is accompanied by a change in the geometry adopted by the macrocycle (30).

As deprotonation and shuttling are thermodynamically coupled (21) the deprotonated rotaxane with M encircling the bipyridinium site, $\mathbf{1}^{2+}$(M⊃bpy^{2+}), is the apparent conjugate base of the starting compound $\mathbf{1}H^{3+}$(M⊃amH$^+$). In particular, it is important to note that the charge-transfer interaction between M and the bpy^{2+} site can occur only in the conjugate base. We hypothesized that upon reduction of the bpy^{2+} unit the ring–axle interaction in the conjugate base could be weakened, while leaving unaffected the hydrogen bonding between M and amH$^+$ in the acid form $\mathbf{1}H^{3+}$, since the macrocycle is relatively far away from the bipyridinium unit. Such a behavior would lead to an increase in the apparent pK_a of the ammonium site that could therefore be affected electrochemically.

Voltammetry. Electrochemical techniques are useful not only to perform the redox switching but also to assess the position of the ring, because the reduction of the bipyridinium unit occurs at more negative potentials when it is surrounded by M (27, 28, 31). Thus, to investigate the interplay of the redox state of the bipyridinium unit and the apparent acidity of the ammonium site we performed cyclic and differential pulse voltammetric experiments in acetonitrile on the rotaxane alone and in the presence of different bases and compared the results with those observed for the axle component $\mathbf{2}H^{3+}$. In all cases two consecutive one-electron reduction processes were detected, corresponding to the bpy^{2+}→bpy$^{(+\cdot)}$ and bpy$^{(+\cdot)}$→bpy$^{(0)}$ reactions (see *SI Appendix*, Figs. S1–S8 and Table S1 for potential values).

The reduction potential values of the axle are only minimally affected by the protonation state of the ammonium station (ΔE_1 = −17 mV, ΔE_2 = −22 mV, Fig. 2*A*), indicating that the electronic and/or conformational communication between the two sites is negligible. In the case of $\mathbf{1}H^{3+}$, the first and second reduction processes (Fig. 2*B*, black trace) occur at the same potential as in the axle (Fig. 2*A*), in agreement with the fact that M encircles amH$^+$ and does not interact with bpy^{2+}. In the presence of 1 equivalent of the strong base phosphazene P_1-*t*-Bu both reduction processes are dramatically shifted to more negative potentials (ΔE_1 = −228 mV, ΔE_2 = −193 mV, Fig. 2*B*). This observation is consistent with the fact that M resides on the bipyridinium unit regardless of its redox state, as previously observed for related rotaxanes with only a bpy^{2+} unit on the axle (32).

Different results are observed if the milder base tributylamine (TBA) is used. First of all, an excess of TBA must be added to afford complete deprotonation of the rotaxane; the equilibrium constant of the reaction shown in Fig. 1 (**B** = TBA) results to be $K = 1.5 \pm 0.3$ (*SI Appendix*, Figs. S8 and S9). The first reduction process of bpy^{2+} becomes chemically irreversible (Fig. 2*C*), with a

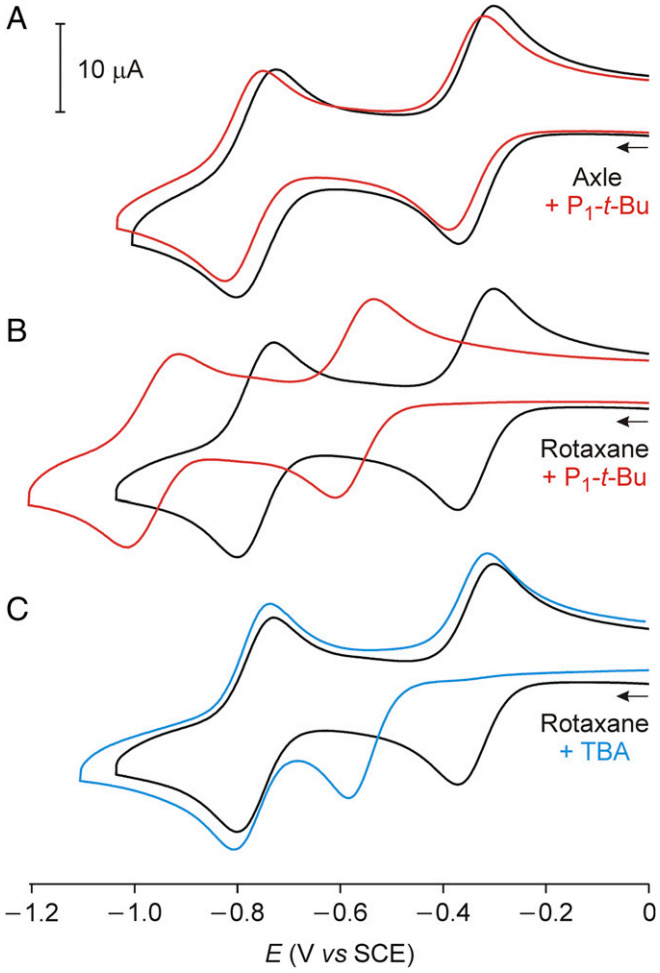

Fig. 2. Cyclic voltammograms (argon-purged CH_3CN/$TEAPF_6$, room temperature, scan rate 300 mV·s^{-1}) of (*A*) the axle component $\mathbf{2}H^{3+}$ and (*B*) rotaxane $\mathbf{1}H^{3+}$ before (black curves) and after addition of 1 equivalent of P_1-*t*-Bu (red curves). (*C*) Cyclic voltammograms of $\mathbf{1}H^{3+}$ before (black curve) and after addition of 22 equivalents of TBA (blue curve). In all cases the base-induced changes are fully reversed upon addition of an equimolar amount of triflic acid.

peak-to-peak separation of 263 mV. The cathodic peak occurs at a significantly more negative potential than for $\mathbf{1}H^{3+}$, at a value similar to that observed upon addition of P_1-*t*-Bu (Fig. 2*B*), whereas the anodic peak take places at nearly the same potential as $\mathbf{1}H^{3+}$ (or $\mathbf{2}H^{3+}$). Such a result suggests that bpy^{2+} is reduced while encircled by M, which successively moves away from the $bpy^{+\cdot}$ site; reoxidation thus occurs on the "free" bipyridinium radical cation. This interpretation is confirmed by the fact that the second reduction process of bpy is reversible and falls at the same potential of $\mathbf{1}H^{3+}$. The same voltammetric pattern is observed in acetone and for scan rates up to 1 $V{\cdot}s^{-1}$ (highest limit for our setup), indicating that the ring shuttling is fast on the time scale of the electrochemical experiment. The electrochemical behavior of the axle $\mathbf{2}H^{3+}$ is identical in the presence of TBA or P_1-*t*-Bu (*SI Appendix*, Figs. S1 and S2).

Since this behavior is not observed in the presence of P_1-*t*-Bu, one must conclude that the TBA base plays a role in the displacement of the ring away from the reduced bipyridinium unit. However, as discussed above, such a displacement could only occur if another recognition site is available on the axle. We have therefore to assume that the amH^+ unit is formed by proton transfer from the conjugate acid $TBAH^+$, accumulated in solution upon initial deprotonation of $\mathbf{1}H^{3+}$ by TBA (Fig. 1, with **B** = TBA). This explanation implies that in the presence of TBA the state $[\mathbf{1}^{2+}(M{\supset}bpy^{2+}) + TBAH^+]$ is more stable than $[\mathbf{1}H^{3+}(M{\supset}amH^+) + TBA]$, in agreement with previous results (Fig. 3, *Top*) (27); upon reduction, however, the relative stabilities of these states are exchanged and $[\mathbf{1}^{(+\cdot)}(M{\supset}bpy^{(+\cdot)}) + TBAH^+]$ becomes less favorable than $[\mathbf{1}H^{+(+\cdot)}(M{\supset}amH^+) + TBA]$ (Fig. 3, *Bottom*).

In such a reversible electrochemical–chemical (EC) mechanism, which is not possible in the free axle, the transfer of an electron triggers the transfer of a proton and requires the shuttling of the macrocycle. Indeed, the inversion of the relative stabilities of protonated and deprotonated states (Fig. 3) takes place because of the presence of the ring, which can return on the ammonium site obtained upon coupled proton transfer from $TBAH^+$, thus restoring more favorable hydrogen-bonding interactions that are energetically advantageous with respect to charge transfer at the reduced $bpy^{(+\cdot)}$ site. However, since part of the energy gain is spent to deprotonate $TBAH^+$, the overall process is allowed only if a mild base such as TBA is employed. In fact, it can be anticipated that the ring-mediated electron–proton transfer should become thermodynamically unfeasible when a stronger base such as P_1-*t*-Bu is used. As shown in Fig. 2*C*, this expectation is fully confirmed by our observations.

From a conceptual point of view, it is important to note that the amine site perceives the modification of the redox state of bpy thanks to the dynamic intramolecular ring shuttling taking place under equilibrium conditions. This remains true also when the destabilization of the bpy site does not actually induce a significant displacement of rings onto the amine site. In fact, in a population of deprotonated rotaxanes the macrocycles remain essentially in the same position (bpy) upon reduction; however, since Brownian fluctuations push the ring back and forth along the axle, the apparent basicity of the amine site increases. Net shuttling will actually be observed only in the presence of a sufficiently strong acid capable of restoring the amH^+ site; in the present case such a process can be electrochemically induced in the presence of $TBAH^+$ but not with P_1-*t*-BuH^+.

EPR Spectroscopy. Further evidence to support the mechanism shown in Fig. 3 could arise from experiments that provide structural information about the reduced rotaxane in the presence of the different bases. NMR spectroscopy is not useful for this purpose because signals are broadened by the presence of the paramagnetic center. On the contrary, insightful information on the $bpy^{(+\cdot)}$ center and its environment can be obtained by EPR spectroscopy. Although this technique constitutes a convenient complement to NMR spectroscopy when paramagnetic centers are involved, its use to characterize radical-containing MIMs is still relatively unexplored (30, 33).

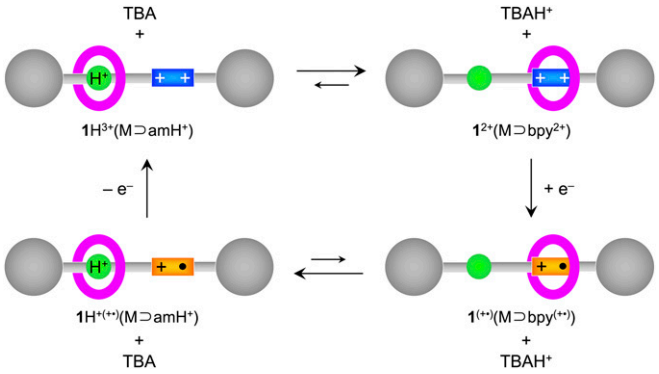

Fig. 3. Schematic representation of the acid–base (horizontal) and electrochemical (vertical) processes observed for rotaxane $\mathbf{1}H^{3+}$ in the presence of TBA. Refer to Fig. 1 for color codes.

Bipyridinium radical cations, $bpy^{(+\cdot)}$, of the rotaxane and its axle component were generated inside the EPR cavity by electrochemical reduction in situ in deoxygenated acetonitrile at room temperature. The EPR spectrum of the radical cation obtained by one-electron reduction of the axle $\mathbf{2}H^{3+}$ (*g*-factor = 2.0031) is shown in Fig. 4*A* (black trace). In keeping with previous studies on the radical cation of the parent 1,1′-dimethyl-4,4′-bipyridinium (34), the spectrum can be well reproduced by assuming the coupling of the unpaired electron with two equivalent N atoms, with a hyperfine coupling constant of 4.17 G, and three groups of four equivalent protons (Fig. 4*A*, red trace). One group is due to the methylene groups of the two chains (aCH_2 4.17 G) and the other two equivalent sets [$a(Ar)H_\alpha$ and $a(Ar)H_\beta$] arise from the aromatic protons (*SI Appendix*, Fig. S10). According to the literature (34), the smaller hyperfine coupling constant for these H atoms can be assigned to the aromatic α-protons (1.24 G), whereas the larger coupling can be assigned to the aromatic β-protons (1.46 G).

An almost identical EPR spectrum was obtained after reduction of the rotaxane $\mathbf{1}H^{3+}$ (Fig. 4*B*), in agreement with the fact that M encircles amH^+ and does not interact with bpy^{2+}. On the contrary, in the presence of 1 equivalent of the strong base P_1-*t*-Bu a substantially different spectral shape was observed (Fig. 4*C*). Specifically, most lines split into an unresolved doublet (highlighted with an asterisk in Fig. 4*C*) that could not be reproduced by considering a symmetric distribution of the spin density between the two heterocyclic rings. Such a nonsymmetric spin distribution suggests that in the deprotonated rotaxane the macrocycle remains located around the bpy unit even when the latter is reduced to the radical cation. The redistribution of spin density on the two pyridine moieties of a bpy unit was recently observed in calixarene-based rotaxanes with a bipyridinium recognition site on the axle (35). Conversely, no changes of the EPR spectral shape were observed upon electrochemical reduction of the axle in the presence of P_1-*t*-Bu (*SI Appendix*, Fig. S10).

The addition of a stoichiometric amount of triflic acid after the treatment with base restored the starting EPR and electrochemical patterns (*SI Appendix*, Figs. S6 and S7), proving the chemical integrity of the various redox forms of the rotaxane in the presence of the base.

When we carried out electrochemical reduction of the rotaxane $\mathbf{1}H^{3+}$ in the presence of an excess of the milder base TBA we observed an EPR spectrum (Fig. 4*D*) almost identical to those observed for the free axle, with or without added base (Fig. 4*A*), or for the rotaxane $\mathbf{1}H^{3+}$ in the absence of base (Fig. 4*B*). Such a result confirms that after the electrogeneration of the $bpy^{(+\cdot)}$ unit in the deprotonated rotaxane M moves away from it and returns on the ammonium site upon coupled proton transfer from $TBAH^+$, thus leading to a symmetric distribution of spin density in the bpy radical cation.

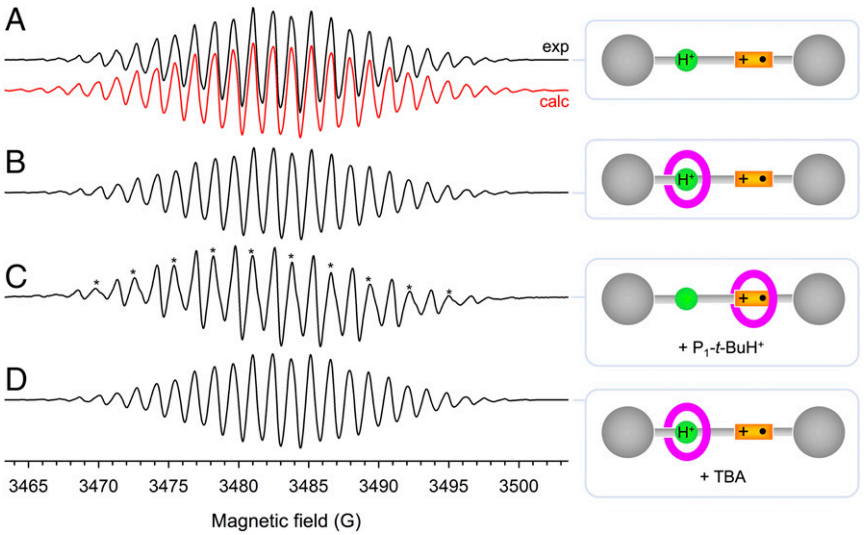

Fig. 4. EPR spectra (black traces) of the bpy radical cation derived from the axle component (*A*) and from the rotaxane before (*B*) and after addition of 1 equivalent of P_1-*t*-Bu (*C*) or 20 equivalents of TBA (*D*). The red trace is the theoretical simulation of spectrum (*A*) obtained by assuming a symmetric distribution of spin density between the two heterocyclic rings of the bpy unit. Conditions: nitrogen-purged $CH_3CN/TBAPF_6$, room temperature. The interpretation of the spectra is schematized in the cartoons; see the text for discussion.

Thermodynamic Analysis. An important consequence of the mechanism shown in Fig. 3, and a key observation for the present discussion, is that the amine site of the rotaxane is more easily protonated when the bipyridinium site is reduced; in other words, the apparent pK_a of amH^+ increases upon reduction of bpy^{2+}. This phenomenon can be quantified by means of thermodynamic considerations based on experimentally determined redox potentials, the equilibrium constant *K* (Fig. 1), and the pK_a values of the bases employed. The situation can be described with the energy-level diagram shown in Fig. 5, which represents schematically all of the states available to the system.

The states explored by the rotaxane differ for (*i*) the base added to the rotaxane and (*ii*) the redox state of the bipyridinium site. The protonation state of the amine/ammonium site depends on these factors, and it is always associated to the position of the macrocycle, that is, the ammonium is always surrounded by the macrocycle and

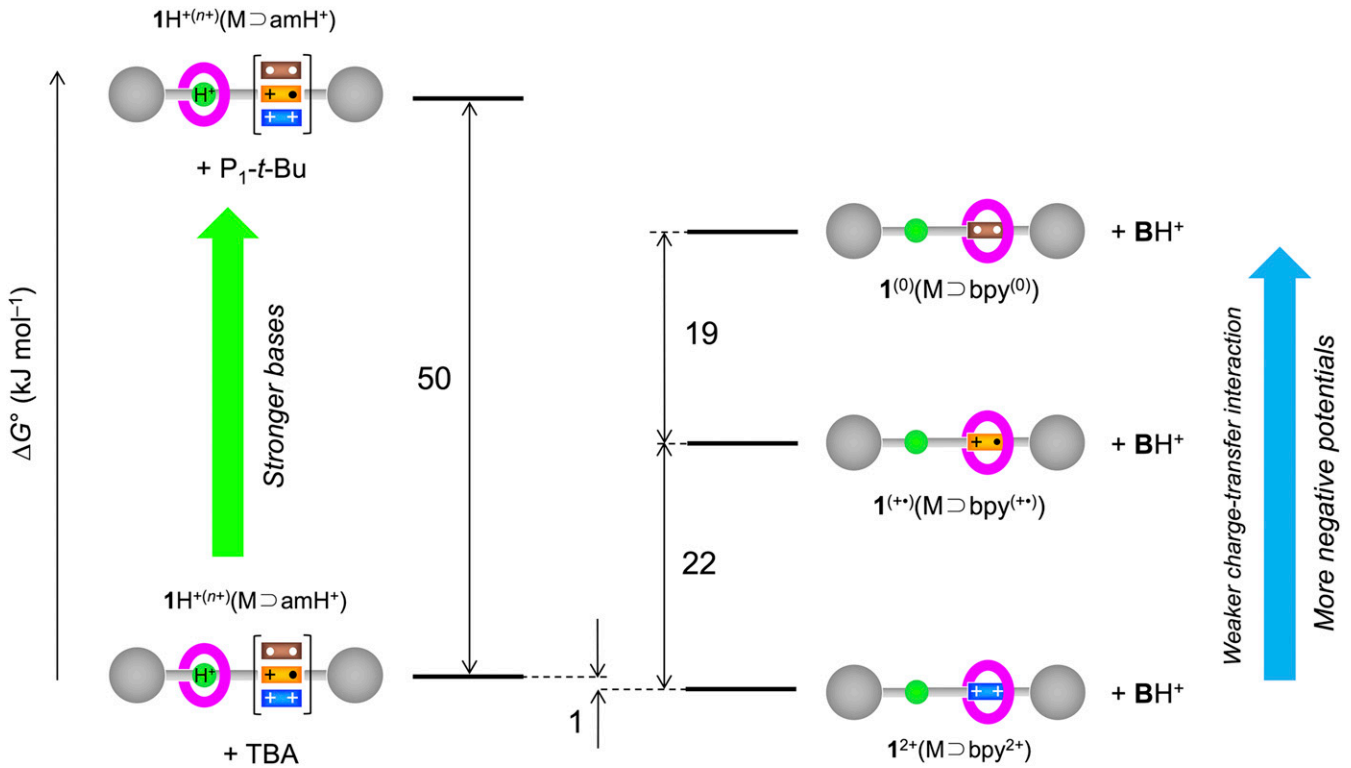

Fig. 5. Simplified energy-level diagram of the accessible states in acetonitrile; refer to Fig. 1 for the color codes of the cartoons. The left-hand side highlights the different strength of the bases added to the rotaxane (the energies of different redox states are offset), whereas the right-hand side represents the different redox states (the energies of different **B**/$\mathbf{BH}^+$ couples are offset; **B** = TBA or P_1-*t*-Bu). See the text and *SI Appendix* for details.

the amine never is. A useful representation of the accessible states can be made by considering relative free energy changes, as discussed below (more detailed considerations are reported in *SI Appendix*).

When comparing different bases, only the difference in their pK_a is considered (Fig. 5, left-hand side); in fact, as it can be reasonably assumed that reduction of the bpy site has a negligible effect on the ammonium-crown ether interaction, the energies of the states with $M{\supset}amH^+$ do not depend on the redox state of bpy. When comparing different redox states, only the energy change associated to the charge-transfer interaction between M and bpy is considered (Fig. 5, right-hand side), because obviously it does not depend on the strength of the base used to deprotonate the rotaxane. Thanks to these rational observations, each side of the diagram depicts the relative stability of the conjugated bases represented (P_1-*t*-Bu and TBA on the left, the three redox forms of the deprotonated rotaxane on the right), and the overall figure provides a prompt perception of the strength of the added base (left-hand side) and the charge-transfer interaction between bpy and M (right-hand side). The two sides can be correlated through the free energy change corresponding to the deprotonation of the rotaxane with TBA, which can be calculated from the equilibrium constant $K = 1.5$ ($\Delta G° = -1.0$ kJ mol^{-1}). From the pK_a value of $TBAH^+$ in acetonitrile (18.26) (36), a pK_a of 18.1 for $\mathbf{1}H^{3+}$ is determined.

The gap of 50 kJ·mol^{-1} between the levels on the left-hand side thus corresponds to the difference in the pK_a values of $TBAH^+$ and P_1-*t*-BuH^+ (26.98 in acetonitrile) (37). The energy increase of 22 kJ·mol^{-1} on going from $[\mathbf{1}^{2+}(M{\supset}bpy^{2+}) + BH^+]$ to $[\mathbf{1}^{(+\cdot)}(M{\supset}bpy^{(+\cdot)}) + BH^+]$ is due to the destabilization of the charge-transfer interaction between bpy and M caused by reduction of the former. This value is estimated from a thermodynamic square cycle involving acid–base and redox reactions that connect the two above mentioned states and the corresponding ones in which M is located on amH^+ (*SI Appendix*, Fig. S12). The reduction potential of $[\mathbf{1}^{2+}(M{\supset}bpy^{2+}) + P_1$-*t*-$BuH^+]$ is experimentally available, and the reduction potential of $[\mathbf{1}H^{3+}(M{\supset}amH^+) + P_1$-*t*-Bu] is equal to that in absence of P_1-*t*-BuH^+. The difference in these reduction potentials, $\Delta E = 0.23$ V, must reflect the difference between the interaction energies of M with bpy^{2+} and $bpy^{(+\cdot)}$ units, $\Delta(\Delta G°) = 22$ kJ·mol^{-1}, and a $pK_a = 22.0$ is obtained for $\mathbf{1}H^{+(+\cdot)}$ (*SI Appendix*). Analogous considerations (*SI Appendix*, Fig. S13) lead us to estimate a destabilization energy of 19 kJ·mol^{-1} for the charge-transfer interaction on going from $bpy^{(+\cdot)}$ to $bpy^{(0)}$, and a $pK_a = 25.4$ for $\mathbf{1}H^{+(0)}$.

The energy diagram shown in Fig. 5 is fully consistent with the experimental evidence. Indeed, the pK_a of $TBAH^+$ (18.26) (36) is intermediate between those of $\mathbf{1}H^{3+}$ and $\mathbf{1}H^{+(+\cdot)}$ (18.1 and 22.0, respectively), leading to the EC scheme depicted in Fig. 3. In contrast, the pK_a of P_1-*t*-BuH^+ (26.98) is always larger than that of the rotaxane regardless of its redox state, giving rise to a chemically reversible reduction behavior (Fig. 2*B*). On switching from $\mathbf{1}H^{3+}$ (stable species at potential values less negative than *ca.* −0.5 V vs. SCE) to $\mathbf{1}H^{+(0)}$ (stable species at potential values more negative than *ca.* −1.2 V vs. SCE), a remarkable overall increase of 7.3 pK_a units is observed.

Conclusions

In summary, we have shown that we can modulate the pK_a of a protonable residue in the axle of a [2]rotaxane by ternary electrochemical switching at a remote site. Reversible pK_a changes exceeding seven units are obtained—to our best knowledge, a significantly larger value than those reported so far for synthetic reversible stimuli-responsive pK_a modulators (38–43). This observation is of general interest because, in principle, pH-sensitive sites with made-to-order pK_a values can be rationally designed using the very same functional group (in the present case, a secondary ammonium) and adjusting the interaction between the ring and a second pH-insensitive site. Effectors different from electrons, such as molecular or ionic substrates, could also be employed for this purpose. Moreover, as the acid–base properties of the pH-sensitive group are determined by its dynamic molecular environment, rotaxanes of this kind can be regarded as models for gaining deeper insight in allosteric communication mechanisms of enzymes. Considering the crucial importance of coupled electron- and proton-transfer processes in natural systems (photosynthesis, respiration, and enzymatic reactions) (3, 44) as well as in technology (fuel cells, sensors, catalysis, and electrochemical devices) (45, 46) the concepts developed here can have far-reaching implications.

Materials and Methods

Chemicals. The investigated compounds were synthesized and characterized in a previous investigation (28). All chemicals were purchased from Aldrich or Fluka and used as received. Small aliquots of TBA, P_1-*t*-Bu, and triflic acid were added in the electrochemical cell from a concentrated acetonitrile solution (typically 40 or 4 mM).

Electrochemical Measurements. Cyclic voltammetric (CV) experiments were carried out at room temperature in argon-purged acetonitrile or acetone with an Autolab 30 multipurpose instrument interfaced to a personal computer using a glassy carbon as the working electrode, a Pt wire as the counterelectrode, and an Ag wire as a quasi-reference electrode. The oxidation wave of ferrocene, added as a standard, was used to calibrate the potential scale and assess electrochemical reversibility. The compounds were examined at a concentration of 4×10^{-4} M, and tetraetylammonium hexafluorophosphate ($TEAPF_6$) 0.04 M was used as the supporting electrolyte. Scan rates from 50 to 1,000 mV·s^{-1} were utilized. Differential pulse voltammograms (DPV) were performed with a scan rate of 20 mV·s^{-1}, a pulse height of 75 mV, and a duration of 40 ms. For reversible processes the same halfwave potential values were obtained from the DPV peaks and from an average of the cathodic and anodic CV peaks. The potential values for not fully reversible processes were estimated from the DPV peaks. The experimental error on the potential values was estimated to be ±10 mV.

EPR Experiments. EPR spectra were recorded at room temperature using an ELEXYS E500 spectrometer equipped with an NMR gaussmeter for the calibration of the magnetic field and a frequency counter for the determination of *g*-factors that were corrected against that of the perylene radical cation in concentrated sulfuric acid ($g = 2.002583$). The homemade electrochemical cell consisted of an EPR flat cell (Wilmad WG-810) equipped with a 25- × 5- × 0.2-mm platinum gauze (cathode) and a platinum wire (anode) (47). The current was supplied and controlled by an AMEL 2051 general-purpose potentiostat. In a typical experiment, the cell was filled with an acetonitrile solution of the appropriate substrate (*ca.* 1 mM) containing tetrabutylammonium hexafluorophosphate ($TBAPF_6$) *ca.* 0.1 M as supporting electrolyte. After thoroughly purging the solution with N_2, spectra were recorded at different potential values in the range from 0 to −1.0 V. An iterative least-squares fitting procedure based on the systematic application of the Monte Carlo method was performed to obtain the experimental spectral parameters of the radical species (48).

ACKNOWLEDGMENTS. This work was supported by the European Research Council under the European Union's Horizon 2020 research and innovation program (Grant 692981), the University of Bologna, and the Centre National de la Recherche Scientifique and the Université Paris Descartes Sorbonne Paris Cité for a "délégation" (B.C.).

1. Traut T (2008) *Allosteric Regulatory Enzymes* (Springer, New York).
2. Motlagh HN, Wrabl JO, Li J, Hilser VJ (2014) The ensemble nature of allostery. *Nature* 508:331–339.
3. Sazanov LA (2015) A giant molecular proton pump: Structure and mechanism of respiratory complex I. *Nat Rev Mol Cell Biol* 16:375–388.
4. Changeux J-P, Edelstein SJ (2005) Allosteric mechanisms of signal transduction. *Science* 308:1424–1428.
5. Kern D, Zuiderweg ERP (2003) The role of dynamics in allosteric regulation. *Curr Opin Struct Biol* 13:748–757.
6. Nussinov R, Tsai C-J (2015) Allostery without a conformational change? Revisiting the paradigm. *Curr Opin Struct Biol* 30:17–24.
7. Lang EJM, Heyes LC, Jameson GB, Parker EJ (2016) Calculated pK_a variations expose dynamic allosteric communication networks. *J Am Chem Soc* 138:2036–2045.
8. Bruns CJ, Stoddart JF (2017) *The Nature of the Mechanical Bond: From Molecules to Machines* (Wiley, Hoboken, NJ).
9. Balzani V, Credi A, Venturi M (2008) *Molecular Devices and Machines: Concepts and Perspectives for the Nanoworld* (Wiley-VCH, Weinheim, Germany).

10. Erbas-Cakmak S, Leigh DA, McTernan CT, Nussbaumer AL (2015) Artificial molecular machines. *Chem Rev* 115:10081–10206.
11. Chung M-K, White PS, Lee SJ, Gagné MR, Waters ML (2016) Investigation of a catenane with a responsive noncovalent network: Mimicking long-range responses in proteins. *J Am Chem Soc* 138:13344–13352.
12. Kremer C, Lützen A (2013) Artificial allosteric receptors. *Chemistry* 19:6162–6196.
13. Cesario M, et al. (1986) Topological enhancement of basicity: Molecular structure and solution study of a monoprotonated catenand. *J Am Chem Soc* 108:6250–6254.
14. Durola F, et al. (2014) Cyclic [4]rotaxanes containing two parallel porphyrinic plates: Toward switchable molecular receptors and compressors. *Acc Chem Res* 47:633–645.
15. Marlin DS, González Cabrera D, Leigh DA, Slawin AMZ (2006) An allosterically regulated molecular shuttle. *Angew Chem Int Ed Engl* 45:1385–1390.
16. Blanco V, Leigh DA, Marcos V, Morales-Serna JA, Nussbaumer AL (2014) A switchable [2]rotaxane asymmetric organocatalyst that utilizes an acyclic chiral secondary amine. *J Am Chem Soc* 136:4905–4908.
17. Galli M, Lewis JEM, Goldup SM (2015) A stimuli-responsive rotaxane-gold catalyst: Regulation of activity and diasteroselectivity. *Angew Chem Int Ed Engl* 54: 13545–13549.
18. Marcos V, et al. (2016) Allosteric initiation and regulation of catalysis with a molecular knot. *Science* 352:1555–1559.
19. Carini M, Da Ros T, Prato M, Mateo-Alonso A (2016) Shuttling as a strategy to control the regiochemistry of bis-additions on fullerene derivatives. *ChemPhysChem* 17: 1823–1828.
20. Eichstaedt K, et al. (2017) Switching between anion-binding catalysis and aminocatalysis with a rotaxane dual-function catalyst. *J Am Chem Soc* 139:9376–9381.
21. Ragazzon G, Credi A, Colasson B (2017) Thermodynamic insights on a bistable acid-base switchable molecular shuttle with strongly shifted co-conformational equilibria. *Chemistry* 23:2149–2156.
22. Cao J, Fyfe MCT, Stoddart JF, Cousins GRL, Glink PT (2000) Molecular shuttles by the protecting group approach. *J Org Chem* 65:1937–1946.
23. Kihara N, Tachibana Y, Kawasaki H, Takata T (2000) Unusually lowered acidity of ammonium group surrounded by crown ether in a rotaxane system and its acylative neutralization. *Chem Lett* 29:506–507.
24. Badjić JD, et al. (2004) A mechanically interlocked bundle. *Chemistry* 10:1926–1935.
25. Romuald C, Busseron E, Coutrot F (2010) Very contracted to extended co-conformations with or without oscillations in two- and three-station [c2]daisy chains. *J Org Chem* 75:6516–6531.
26. Nakazono K, Takata T (2010) Neutralization of a sec-ammonium group unusually stabilized by the "rotaxane effect": Synthesis, structure, and dynamic nature of a "free" sec-amine/crown ether-type rotaxane. *Chemistry* 16:13783–13794.
27. Ashton PR, et al. (1998) Acid-base controllable molecular shuttles. *J Am Chem Soc* 120: 11932–11942.
28. Schäfer C, et al. (2015) An artificial molecular transporter. *ChemistryOpen* 5:120–124.
29. Garaudée S, et al. (2005) Shuttling dynamics in an acid-base-switchable [2]rotaxane. *ChemPhysChem* 6:2145–2152.
30. Franchi P, et al. (2016) Structural changes of a doubly spin-labeled chemically driven molecular shuttle probed by PELDOR spectroscopy. *Chem Eur J* 22:8745–8750.
31. Badjic JD, et al. (2006) Operating molecular elevators. *J Am Chem Soc* 128:1489–1499.
32. Altobello S, Nikitin K, Stolarczyk JK, Lestini E, Fitzmaurice D (2008) Quantitative conformational study of redox-active [2]rotaxanes, part 1: Methodology and application to a model [2]rotaxane. *Chemistry* 14:1107–1116.
33. Coskun A, et al. (2011) Mechanically stabilized tetrathiafulvalene radical dimers. *J Am Chem Soc* 133:4358–4547.
34. Benniston AC, et al. (2007) A spectroscopic study of the reduction of geometrically restrained viologens. *Chemistry* 13:7838–7851.
35. Zanichelli V, et al. (2016) Synthesis and characterization of constitutionally isomeric oriented calix[6]arene-based rotaxanes. *Eur J Org Chem* 1033–1042.
36. Coetzee JF, Padmanabhan GR (1965) Properties of bases in acetonitrile as solvent. IV. Proton acceptor power and homoconjugation of mono- and diamines. *J Am Chem Soc* 87:5005–5010.
37. Kaljurand I, et al. (2005) Extension of the self-consistent spectrophotometric basicity scale in acetonitrile to a full span of 28 pK_a units: Unification of different basicity scales. *J Org Chem* 70:1019–1028.
38. Kawai SH, Gilat SL, Lehn J-M (1999) Photochemical pK_a-modulation and gated photochromic properties of a novel diarylethene switch. *Eur J Org Chem* 2359–2366.
39. Peters MV, Stoll RS, Kühn A, Hecht S (2008) Photoswitching of basicity. *Angew Chem Int Ed Engl* 47:5968–5972.
40. Ray D, Foy JT, Hughes RP, Aprahamian I (2012) A switching cascade of hydrazone-based rotary switches through coordination-coupled proton relays. *Nat Chem* 4: 757–762.
41. Abeyrathna N, Liao Y (2015) A reversible photoacid functioning in PBS buffer under visible light. *J Am Chem Soc* 137:11282–11284.
42. Weston CE, Richardson RD, Fuchter MJ (2016) Photoswitchable basicity through the use of azoheteroarenes. *Chem Commun (Camb)* 52:4521–4524.
43. Utley JHP, Folmer Nielsen M, Wyatt P (2016) Electrogenerated bases and nucleophiles. *Organic Electrochemistry*, eds Hammerich O, Speiser B (CRC, Boca Raton, FL), 5th Ed, pp 1625–1656.
44. Weinberg DR, et al. (2012) Proton-coupled electron transfer. *Chem Rev* 112: 4016–4093.
45. Zhang H, Shen PK (2012) Recent development of polymer electrolyte membranes for fuel cells. *Chem Rev* 112:2780–2832.
46. Costentin C, Robert M, Savéant J-M, Tard C (2014) Breaking bonds with electrons and protons. Models and examples. *Acc Chem Res* 47:271–280.
47. Alberti A, et al. (2000) Phosphoryl- and thiophosphoryl-dithioformates. Part IV. Electrochemical reduction and EPR study of the radical anions. *J Chem Soc Perkin Trans 2* 1908–1913.
48. Franchi P, Mezzina E, Lucarini M (2014) SOMO-HOMO conversion in distonic radical anions: An experimental test in solution by EPR radical equilibration technique. *J Am Chem Soc* 136:1250–1252.